

Hydrogen-Stuffed, Quartz-like Water Ice

Timothy A. Strobel,^{*,†} Maddury Somayazulu,[†] Stanislav V. Sinogeikin,[‡] Przemyslaw Dera,[§] and Russell J. Hemley^{||,⊥}

[†]Geophysical Laboratory, Carnegie Institution of Washington, Washington, D.C. 20015, United States

[‡]HPCAT, Geophysical Laboratory, Carnegie Institution of Washington, Argonne, Illinois 60439, United States

[§]Hawaii Institute of Geophysics and Planetology, School of Ocean and Earth Science and Technology, University of Hawaii at Manoa, Honolulu, Hawaii 96822, United States

^{||}Department of Civil and Environmental Engineering, George Washington University, Washington, D.C. 20052, United States

[⊥]Lawrence Livermore National Laboratory, Livermore, California 94550, United States

S Supporting Information

ABSTRACT: Through use of *in situ* Raman spectroscopy and single-crystal/powder X-ray diffraction, we resolve the “C₀” phase structure discovered recently in the H₂ + H₂O system. This phase forms at ∼400 MPa and 280 K with the nominal composition (H₂O)₂H₂ and three formula units per unit cell. The hexagonal structure is chiral, consisting of interpenetrating spiral chains of hydrogen-bonded water molecules and rotationally disordered H₂ molecules, and shows topological similarities with the mineral quartz. Like other clathrate hydrates and forms of ice, the protons of H₂O molecules within C₀ are disordered. The large zeolite-like channels accommodate significant amounts of hydrogen (5.3% by weight) in a unique hydrogen-bonded lattice, which might be applicable to the thermodynamic conditions found on icy planetary bodies.

The tetrahedral nature of water connected by hydrogen bonding gives rise to a complex phase diagram with 17 crystalline phases known at present, most of which are formed by the application of pressure.^{1,2} Similarly, numerous silicate polymorphs are known, and strong parallels can be drawn between the packing of tetrahedra and network topologies found in H₂O and SiO₂ phases.³ For example, tridymite and cristobalite are analogues of ice I_h and I_c, respectively,⁴ while low-energy hypothetical ice analogues of quartz have been predicted theoretically.^{4,5} These structural analogies extend to various types of clathrate structures—guest/host, zeolite-like compounds that form when water crystallizes in the presence of small atoms or molecules.⁶ For the binary H₂ + H₂O system, three clathrate compounds with resolved structures are presently known. Structure two (sII, zeolite-type MTN) clathrate hydrate is composed of two types of polyhedral water cages, the larger and smaller of which can hold up to four and one hydrogen molecules, respectively.⁷ Fully loaded sII clathrate has a H₂:H₂O ratio of 1:2.83, and the melting/dissociation curve has a positive Claperon slope extending from ∼150 K at 1 atm to 275 K at ∼400 MPa.^{7,8} Clathrate one (C₁) is a filled form of ice II with an ideal H₂:H₂O ratio of 1:3.⁹ The melting curve of C₁ extends from 300 K at 700 MPa to 390 K at 2 GPa. Clathrate two (C₂) consists of two interpenetrating diamond lattices and represents a filled

form of cubic ice (I_c) with an ideal H₂:H₂O ratio of 1:1. C₂ forms above 2 GPa at room temperature.⁹

Significant structural diversity is observed between the three established binary phases, yet large regions of the H₂-H₂O phase diagram remain completely unexplored. In addition to its fundamental importance in chemistry, this binary system is of great interest for planetary science¹⁰ as well as potential energy applications.¹¹ A study combining low temperature with high pressure indicated that all three of these phases are stable at low temperature, but a new phase appears between the stability conditions of sII and C₁.¹² The structure of this phase could not be resolved, but preliminary indexing suggested it could be related to sT clathrate¹³ or an analogue of quartz. Similarly, Efimchenko et al.¹⁴ reported the same phase (giving the name C₀) and proposed a unique trigonal structure based on preliminary powder diffraction data with variable intensity between three samples. The presence (and correct position) of a partially occupied oxygen atom within this structure was postulated to originate from entrapped N₂ by Smirnov and Stegailov,¹⁵ as these samples were all processed *ex situ* in liquid nitrogen. Meanwhile, computational predictions of this system suggest that several compounds could be energetically stable under high-pressure conditions. Using *ab initio* searching methods, Qian et al.¹⁶ calculated two stable “C₀” structures (one monoclinic and one trigonal) below 1 GPa and confirmed the stabilities of C₁ and C₂ at higher pressure. Smirnov and Stegailov¹⁵ used classical molecular dynamics (MD) calculations to determine that sT clathrate and a variant of the structure proposed by Efimchenko et al.¹⁴ (one without the 1/2 occupied oxygen) could both be viable candidates for C₀. Here we resolve these issues and report an accurate structural model of this phase based on *in situ* Raman spectroscopy combined with single-crystal and powder synchrotron X-ray diffraction (XRD). We find a unique hydrogen-filled, ice-based chiral structure with oxygen topology very similar to the mineral quartz and other, as-of-yet-hypothetical, three-dimensional nets.

Binary H₂ + H₂O samples were loaded into diamond anvil cells allowing for *in situ* Raman and diffraction studies (see Supporting Information (SI)). We first describe the Raman spectra, which

Received: July 6, 2016

Published: August 19, 2016

provide important structural constraints based on intrinsic vibrational/rotational excitations. The low-frequency region between $\sim 100\text{--}1000\text{ cm}^{-1}$ contains information regarding the rotational excitations of H_2 ($S_{\nu=0}(J)$, where ν is the vibrational quantum number and J is the initial rotational quantum number for $\Delta J = \pm 2$ transitions) as well as lattice phonons of the hydrogen-bonded water host. By comparing the roton spectra of C_0 with sII and C_1 , two structures in which H_2 rotates freely,^{9,17} we can see that H_2 molecules within C_0 also act as essentially free quantum rotors (Figure 1a). Increased broadening of the $S_0(J)$

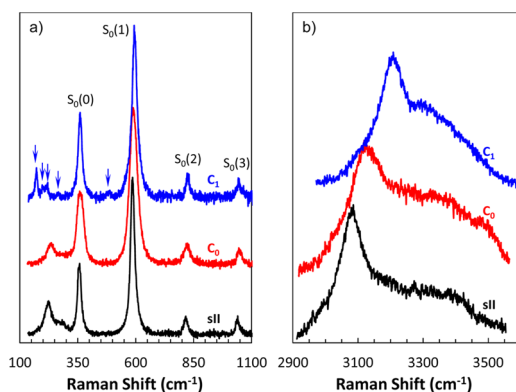


Figure 1. (a) Raman spectra of the H_2 roton and lattice phonon region and (b) OH stretching region. All spectra were obtained at $260 \pm 5\text{ K}$ and pressures of 0.3, 0.5, and 1.5 GPa for sII, C_0 , and C_1 , respectively. Arrows indicate sharp lattice phonons in C_1 .

lines could indicate enhanced interactions with the H_2O lattice or increased disorder. For proton-disordered phases like I_h and sII, broad lattice phonons are observed near 220 cm^{-1} .^{17,18} This is in contrast with ordered phases like ice II and C_1 , which exhibit sharp phonon bands due to the ordering of water H atoms on discrete lattice positions.⁹ The sII-like lattice phonons observed for C_0 clearly indicate that this phase is also proton disordered, and we can expect a quasi-tetrahedral arrangement of H atoms surrounding each O atom with 50% probability at each site.

The principal peak of the OH stretching region shows a clear shift to higher frequency going from sII to C_0 to C_1 . It is well-known that OH frequencies are correlated with $\text{O}\cdots\text{O}$ distances due to increased hydrogen bonding, which eventually leads to bond symmetrization at higher densities.¹⁹ From the frequency shift with structure (and pressure), we can expect that $\text{O}\cdots\text{O}$ distances in C_0 are slightly expanded compared with those found in sII at similar conditions, but less than the distances found in C_1 .

The H_2 vibrons [$Q(J)$] provide important information as to the nature of trapped H_2 . The vibron spectrum of sII clathrate shows a range of peaks due to a distribution of occupancies between small and large cages (Figure 2).^{17,20} For filled ice phases, like C_1 and C_2 , only a single vibron peak is present due to the single crystallographic site available within these structures that do not contain discrete polyhedral cavities.^{9,12} The spectra for C_0 also show a single Raman peak, and by analogy, we conclude that this phase is filled-ice-like, containing only a single crystallographic site without multiply occupied polyhedral cavities. Clear stepwise changes in the vibron frequency with pressure delineate phase transition boundaries, but likely include some degree of overpressurization. These discrete regions serve as clear markers to distinguish between structures and also allow

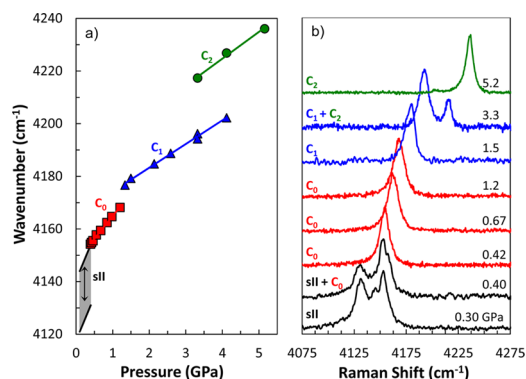


Figure 2. (a) H_2 Raman stretching frequency as a function of pressure and (b) vibron spectral features at $260(\pm 5)\text{ K}$. The shaded gray region for sII indicates a range of frequencies present due to multiply occupied cages.

us to confirm that the low-frequency and OH contributions (as in Figure 1) are from pure single phases.

With this understanding from spectroscopic observations, we now turn to the single-crystal XRD data. By cycling the temperature near the liquidus, we were able to produce several crystals suitable for *in situ* synchrotron single-crystal diffraction. At 400 MPa and 280 K, these data were readily indexed to a hexagonal lattice with $a = 6.285(4)\text{ \AA}$ and $c = 6.213(6)\text{ \AA}$.²¹ The possibility for a tetragonal structure (such as sT clathrate) was immediately ruled out, and space groups $P6_322$ and $P6_122$ were identified as the best candidates (see SI). These space groups are in contrast with the trigonal ones proposed by Efimchenko et al. based on powder data,¹⁴ but can be still be classified as enantiomorphic (chiral) pairs that differ only in the direction of a screw axis, making it impossible to distinguish with our X-ray data.

The initial structural solution was obtained considering only oxygen atomic positions since the intensity scattered from O is expected to dominate the observed diffraction intensities. The structure contains six O atoms per unit cell (on the 6b Wyckoff positions). With only O atoms present, the model refined to a reasonable R1 value of 5.5% using Shexl.²² With the O positions determined, and knowing that the protons are disordered from the Raman data, we manually added covalently bound hydrogens along vectors connecting all adjacent O atoms at a distance of 0.96 \AA from the origin. By adding H atoms at these fixed 12c positions, R1 dropped to 3.9%.

Structural examination shows that the H-bonded network forms large channels along the crystallographic c -axis, leaving the 6a Wyckoff position available for rotationally disordered H_2 molecules, which is fully consistent with the single-site, filled-ice-like structure inferred from Raman measurements. Within the $P6_322$ model, this 6-fold H_2 site must be partially occupied to avoid unphysical $\text{H}_2\text{--H}_2$ distances and an unphysical total compound volume (discussed below). An ideal occupancy of 50% provides a physical meaning of two configurations possible (indicated by blue and green spheres in Figure 3). This additional disorder can be understood as a consequence of the disordered water protons that are the nearest neighbors to the H_2 molecules. The $\text{O--H}\cdots\text{H}_2$ distance can fluctuate depending on specific water proton configurations, giving rise to two channel configurations with equal probability. After refining the enclathrated H_2 molecules (as He atoms with large isotropic displacements), the R1 value dropped again to 2.6%.

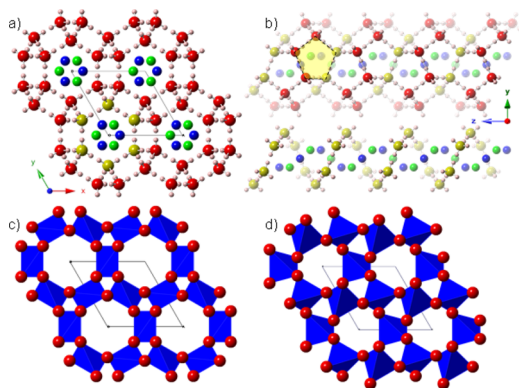


Figure 3. (a) Structure of C_0 . Large red and small pink spheres indicate water O and H atoms, respectively, while blue and green spheres indicate disordered H_2 molecules, which are 50% occupied. (b) Pentagonal tiling of channels down the c -axis and isolated spiral chain with O atoms emphasized in yellow. (c) Polygon view of C_0 compared with the structure of quartz (d). Distorted blue tetrahedra in C_0 represent void space, whereas blue tetrahedra for quartz represent silicon atoms.

The resulting structure consists of interpenetrating spiral chains of hydrogen-bonded water molecules surrounding rotationally disordered H_2 molecules along the crystallographic c -axis (Figure 3). Interconnected spiral chains of H-bonded waters form atomic-scale tubes whose sides are completely tiled by pentagonal faces (Figure 3b). The entire H-bonded network is, in fact, constructed solely by five-membered rings. H_2 molecules spiral through the channels along the screw axis, but are translationally out of phase with the central H_2O chain. Water molecules from six adjacent helices with hexagonal packing complete each channel and its pentagonal tiling. Interatomic $O1\cdots O1$ distances range between 2.76 and 2.78 Å, while $O1\cdots O1\cdots O1$ (and H–O–H by constraint) angles vary between 104.5° and 124.7° . These distances and angles are well in line with acceptable values for known ice and clathrate phases¹ and are also in accordance with the Raman data that impose $O\cdots O$ distances to be intermediate between *sII* and C_1 .

The C_0 structure contains similarities with the structure of low (α) quartz, long considered a possible framework for pure H_2O ice.³ As another chiral structure, quartz crystallizes in both $P3_221$ and $P3_121$, two of the original candidate space groups for C_0 . While not strictly isostructural, quartz also contains six topologically equivalent oxygen atoms per unit cell on the $6c$ positions, which can be distorted slightly into the C_0 positions (Figure 3c,d). Although the oxygen topology is equivalent, oxygen is not the tetrahedral species in quartz. Thus, the critical difference between these two structures is the absence of the silicon position in the C_0 phase: hydrogen atoms bridge four-coordinate oxygen atoms along the absent vertices that comprise silicon tetrahedra found in quartz. The topology of this oxygen framework is also very similar to the preliminary model proposed by Efimchenko et al.¹⁴ based on powder XRD data, but without the partially occupied oxygen position. In addition, our model requires only one crystallographically unique oxygen atom, whereas two are required for the $P3_121$ structure.

Based on our structural model, the nominal composition of the C_0 phase is $(H_2O)_2H_2$ (three formula units per cell) assuming half occupancy of H_2 positions. Efimchenko et al.¹⁴ suggested a lower-bound $H_2:H_2O$ molar ratio of 0.13 based on gas release measurements where H_2 was observed to leave to C_0 phase immediately upon heating above 77 K. The *in situ* composition

near $1H_2:2H_2O$ is supported by volumetric arguments. By assuming molar volumes for the individual components and adding them in the compound stoichiometric ratio, thermodynamics dictates that the total volume must be less than the individual components at their respective conditions. But this estimate should be reasonably close in magnitude to the true compound volume in the absence of unusually strong interactions. At 400 MPa and 280 K, hydrogen exists as a supercritical fluid with a molecular volume of $33.38 \text{ \AA}^3/H_2$ and H_2O exists as liquid with a molecular volume $26.40 \text{ \AA}^3/H_2O$.²³ Taking $6H_2O + 3H_2$ at these conditions gives a total volume of 258.5 \AA^3 compared with 212.5 \AA^3 for the actual compound. This agreement conforms to the requirement of lower compound volume, but we also recall that H_2 molecules within clathrate phases are significantly compressed as compared with the fluid phase. H_2-H_2 distances in *sII* clathrate at 1 atm are in fact equivalent to solid H_2-H_2 extrapolated distances at 1.7 GPa.^{7,24} By assuming a H_2 volume derived from distances found in *sII* clathrate ($17.93 \text{ \AA}^3/H_2$), an atomic water volume of $26.45 \text{ \AA}^3/H_2O$ is required to obtain the total C_0 volume, which is in between the atomic volumes of ice I_h and ice II .¹

As a final test of our structural model, we calculate diffraction intensities from a powder C_0 sample obtained by rapid cooling at 0.7 GPa (Figure 4). Rietveld refinement was performed using

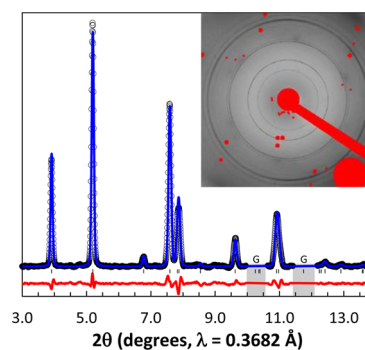


Figure 4. Rietveld refinement of powder XRD at 0.7 GPa and 170 K. Points indicate data, while blue and red lines show the Rietveld model ($R_{wp} = 10.17\%$) and difference, respectively. Portions not refined (gray bars) due to strong scattering from the gasket (G) material. Inset shows measured 2D data with homogeneous powder statistics.

GSAS with EXPGUI.^{25,26} The atomic positions and displacement parameters were used directly from the single crystal model. Only the lattice parameters, background, and three peak profile terms were refined (GW, GU, LX, GSAS profile type 2). The increased pressure resulted in decreased lattice parameters of $a = 6.2279(2) \text{ \AA}$ and $c = 6.1816(4) \text{ \AA}$. Nevertheless, this quantitative agreement between observation and model indicates a robust structural solution.

Additional support for this structural model comes from recent theoretical calculations. Qian et al.¹⁶ predicted a similar structure of the same composition, but in space group $P3_2$ and with ordered water protons. Nevertheless, the O atom topology is nearly identical, and finite temperature effects can account for differences in the nature of the hydrogen atoms and overall disorder resulting in higher time/space-averaged symmetry as measured by diffraction. MD simulations also suggest that this configuration is energetically stable at 300 K on the longest time scales (10's of ns) tested.¹⁵

We comment on several limitations of our present analysis. The samples are largely dominated by H atoms, which are not

very amenable to X-ray scattering, and the completeness of the single-crystal data sets were limited due to intrinsic constraints on the cell and cryostat opening angles. While we are confident in the general configuration of O atoms and can identify, with some certainty, the H atom locations based on Raman scattering, chemical intuition and agreement with theoretical predictions, neutron scattering experiments would be valuable to solve the final structure. We note that H positions were only inferred for C₁ and C₂ structures as well, but recent developments in *in situ* neutron scattering under pressure should make studying all of these systems feasible in the immediate future.²⁷

Despite the above limitations, our identification of the overall structure and the resulting chemical picture are robust. It is interesting to note that C₀ takes on similarities with the structure of quartz. While quartz is a major silicate mineral found on earth, C₀ might be a topologically related water-based mineral found in abundance on icy planetary bodies. We note also that the topology of O atoms and crystallographic space group for C₀ are identical to the chiral framework structure predicted for pure silicon and other hypothetical four-coordinated nets.^{28,29}

In summary, a quartz-like structure for (H₂O)₂H₂ is established on the basis of Raman spectroscopy combined with single-crystal and powder XRD. The compound highlights the structural diversity found within hydrogen-bonded frameworks and related four-coordinated systems, and how that diversity is enhanced by the presence of guest molecules in the structure. In view of the abundance of H₂ and H₂O in the cosmos and the observed *P–T* stability of the compound, the material may be found at modest depths within icy planetary bodies. Because interactions between H₂ and H₂O at these conditions are largely dispersive in nature, we predict that this C₀ phase structure will also be found in mixtures with other small molecules or atoms, like He or Ne. Its significant hydrogen content and large channels that give rise to enhanced H₂ mobility may also facilitate practical applications of the material for hydrogen storage.

■ ASSOCIATED CONTENT

⊕ Supporting Information

The Supporting Information is available free of charge on the ACS Publications website at DOI: 10.1021/jacs.6b06986.

Methods and supporting structural information (PDF)

■ AUTHOR INFORMATION

Corresponding Author

*tstrobels@ciw.edu

Notes

The authors declare no competing financial interest.

■ ACKNOWLEDGMENTS

We thank D.Y. Kim for valuable discussions and anonymous reviewers for insightful comments. This work was supported by EFree, an Energy Frontier Research Center funded by the U.S. Department of Energy (DOE) Office of Science, Basic Energy Sciences (BES), under grant no. DE-SC0001057. Portions of this work were performed at HPCAT (Sector 16), Advanced Photon Source (APS), Argonne National Laboratory. HPCAT operations are supported by DOE-NNSA under award no. DE-NA0001974 and DOE-BES under award no. DE-FG02-99ER45775, with partial instrumentation funding by NSF. The Advanced Photon Source is a U.S. DOE Office of Science User Facility operated for the DOE Office of Science by Argonne National Laboratory under contract no. DE-AC02-06CH11357.

Work at LLNL was performed under the auspices of the U.S. DOE under contract no. DE-AC52-07NA27344.

■ REFERENCES

- (1) Petrenko, V. F.; Whitworth, R. W. *Physics of Ice*; Oxford University Press: Oxford, 1999.
- (2) Falenty, A.; Hansen, T. C.; Kuhs, W. F. *Nature* **2014**, *516*, 231.
- (3) Bernal, J. D.; Fowler, R. H. *J. Chem. Phys.* **1933**, *1*, 515.
- (4) Tribello, G. A.; Slater, B.; Zwijnenburg, M. A.; Bell, R. G. *Phys. Chem. Chem. Phys.* **2010**, *12*, 8597.
- (5) Svishchev, I. M.; Kusalik, P. G. *Phys. Rev. B: Condens. Matter Mater. Phys.* **1996**, *53*, R8815.
- (6) Sloan, E. D.; Koh, C. A. *Clathrate Hydrates of Natural Gases*, 3rd ed.; CRC Press: Boca Raton, FL, 2008.
- (7) Lokshin, K. A.; Zhao, Y. S.; He, D. W.; Mao, W. L.; Mao, H. K.; Hemley, R. J.; Lobanov, M. V.; Greenblatt, M. *Phys. Rev. Lett.* **2004**, *93*, 125503.
- (8) Dyadin, Y. A.; Larionov, E. G.; Manakov, A. Y.; Zhurko, F. V.; Aladko, E. Y.; Mikina, T. V.; Komarov, V. Y. *Mendeleev Commun.* **1999**, *9*, 209.
- (9) Vos, W. L.; Finger, L. W.; Hemley, R. J.; Mao, H. K. *Phys. Rev. Lett.* **1993**, *71*, 3150.
- (10) Sandford, S. A.; Allamandola, L. J.; Geballe, T. R. *Science* **1993**, *262*, 400.
- (11) Strobel, T. A.; Hester, K. C.; Koh, C. A.; Sum, A. K.; Sloan, E. D. *Chem. Phys. Lett.* **2009**, *478*, 97.
- (12) Strobel, T. A.; Somayazulu, M.; Hemley, R. J. *J. Phys. Chem. C* **2011**, *115*, 4898.
- (13) Hirai, H.; Tanaka, T.; Kawamura, T.; Yamamoto, Y.; Yagi, T. *J. Phys. Chem. Solids* **2004**, *65*, 1555.
- (14) Efimchenko, V. S.; Kuzovnikov, M. A.; Fedotov, V. K.; Sakharov, M. K.; Simonov, S. V.; Tkacz, M. *J. Alloys Compd.* **2011**, *509*, S860.
- (15) Smirnov, G. S.; Stegailov, V. V. *J. Phys. Chem. Lett.* **2013**, *4*, 3560.
- (16) Qian, G.-R.; Lyakhov, A. O.; Zhu, Q.; Oganov, A. R.; Dong, X. *Sci. Rep.* **2014**, *4*, 5606.
- (17) Strobel, T. A.; Sloan, E. D.; Koh, C. A. *J. Chem. Phys.* **2009**, *130*, 014506.
- (18) Giannasi, A.; Celli, M.; Ulivi, L.; Zoppi, M. *J. Chem. Phys.* **2008**, *129*, 084705.
- (19) Goncharov, A. F.; Struzhkin, V. V.; Somayazulu, M. S.; Hemley, R. J.; Mao, H. K. *Science* **1996**, *273*, 218.
- (20) Mao, W. L.; Mao, H. K.; Goncharov, A. F.; Struzhkin, V. V.; Guo, Q. Z.; Hu, J. Z.; Shu, J. F.; Hemley, R. J.; Somayazulu, M.; Zhao, Y. S. *Science* **2002**, *297*, 2247.
- (21) Dera, P.; Zhuravlev, K.; Prakapenka, V.; Rivers, M. L.; Finkelstein, G. J.; Grubor-Urosevic, O.; Tschauner, O.; Clark, S. M.; Downs, R. T. *High Pressure Res.* **2013**, *33*, 466.
- (22) Sheldrick, G. M. *Acta Crystallogr., Sect. C: Struct. Chem.* **2015**, *71*, 3.
- (23) Lemmon, E. W.; McLinden, M. O.; Friend, D. G. *NIST Chemistry WebBook*, NIST Standard Reference Database Number 69; NIST: Gaithersburg, MD (accessed June 2016).
- (24) Hemley, R. J.; Mao, H. K.; Finger, L. W.; Jephcoat, A. P.; Hazen, R. M.; Zha, C. S. *Phys. Rev. B: Condens. Matter Mater. Phys.* **1990**, *42*, 6458.
- (25) Larson, A. C.; Von Dreele, R. B. *General Structure Analysis System (GSAS)*; Los Alamos National Laboratory: Los Alamos, NM, 2000.
- (26) Toby, B. H. *J. Appl. Crystallogr.* **2001**, *34*, 210.
- (27) Boehler, R.; Guthrie, M.; Molaison, J. J.; dos Santos, A. M.; Sinogeikin, S.; Machida, S.; Pradhan, N.; Tulk, C. A. *High Pressure Res.* **2013**, *33*, 546.
- (28) Pickard, C. J.; Needs, R. J. *Phys. Rev. B: Condens. Matter Mater. Phys.* **2010**, *81*, 014106.
- (29) O'Keefe, M. *Phys. Chem. Chem. Phys.* **2010**, *12*, 8580.